

Modeling unmanned aerial vehicle jet ignition wankel engines with CAE/CFD

Albert Boretti*

Department of Mechanical and Aerospace Engineering (MAE), Benjamin M. Statler College of Engineering and Mineral Resources, West Virginia University (WVU), P.O. Box 6106, 325 Engineering Sciences Building, Morgantown, WV 26506, USA

(Received March 4, 2015, Revised April 8, 2015, Accepted April 8, 2015)

Abstract. The paper presents some details of the CFD modeling of a novel design where jet ignition devices replace the traditional spark plugs for a faster and more complete combustion. The numerical simulations show how the pre-chamber jet ignition in a Wankel engine differs from reciprocating piston engine applications. The jets issuing from the jet ignition pre-chamber have many different speeds in the different directions as the pressure build-up at the trailing edge of the rotating chamber makes extremely fast the ignition of the chamber mixture in the direction of rotation. Conversely it prevents the jet ignition in the opposite direction. Careful positioning along the periphery and design of the connecting pipes and the pre-chamber volume with the help of CFD simulations permits to achieve extremely fast and complete combustion as impossible with spark plugs. The paper proposes results of CFD simulations of the combustion evolution within a jet ignited Wankel engine rotor, detailing challenges and opportunities of the application, as well as a first assessment of the impact the faster and more complete combustion permitted by jet ignition may have on the performances of Wankel engines for unmanned aerial vehicles applications.

Keywords: unmanned aerial vehicles; wankel engines; CFD simulations; CAE simulations

1. Introduction

The Wankel engine is an Internal Combustion Engine (ICE) using an eccentric rotary design. This design provides benefits of simplicity, smoothness, compactness, high engine speeds and high power to weight and power to displaced volume ratio vs. the traditional four-stroke engine design with reciprocating pistons (Sherman 2008, Ohkubo *et al.* 2004, Jones 1979, Danieli *et al.* 1974, Shimizu *et al.* 1995, Yamamoto *et al.* 1972, Izweik 2009).

Felix Wankel received his first patent for the Wankel engine in 1929. The first development began in 1951. NSU started development of the Wankel engine, actually of two variants, the DKM and the KKM, in 1951. First prototypes were finally built in 1957 (Sherman 2008). Starting 1960, many manufacturers signed licence agreements with NSU, including Curtiss-Wright and Mazda. NSU and Mazda competed to bring the first Wankel car to market. The NSU spider of 1964 was the first Wankel car for sale, followed by the NSU Ro-80 of 1967 and the Mazda Cosmo 110s also

*Corresponding author, Professor, E-mail: a.a.boretti@gmail.com; alboretti@mail.wvu.edu

of 1967.

While NSU did not produce any reliable apex seals of the rotor, Mazda did, and the Cosmo was followed by a number of other designs even if ultimately Mazda concentrated only on sport cars, with the famous RX-7 1978-2002 and the RX-8 of 2003-2012. The engines were mostly twin rotor natural aspirated or turbocharged in the RX-7, and naturally aspirated in the RX-8. The third generation sequential twin-turbocharged RX-7 was one of the most fascinating sport cars. The more family oriented naturally aspirated RX-8 had the Renesis engine delivering better fuel economy, reliability and emissions than any other automotive rotary engine.

As the combustion within the Wankel was always incomplete, a thermal reactor on the exhaust was proposed by Mazda in 1973 to address the issue and meet emission standards at the price of increased fuel consumption. Despite the thermal reactor system was considerably improved in the first generation of RX-7 in 1978, Mazda then shifted to the more expensive but more efficient catalytic converter to control the pollutant emissions in the following RX-7 and the RX-8. The relatively low fuel conversion efficiency was the major issue of the latest RX-8 that the jet ignition innovation is aimed to solve.

The four-stroke cycle events occur in a moving combustion chamber between the inside of an epitrochoid shaped housing and a triangular rotor with bow-shaped flanks. Seals at the corners of the rotor close against the periphery of the housing, dividing it into three moving combustion chambers per rotor or lobes. Every rotor revolutions there are three power strokes. The central eccentric drive shaft (the E-shaft) passes through the center of the rotor and is supported by fixed bearings. The rotor moves 1 turn for 3 turns of the E-shaft that is revving three times faster. Wankel engines have much higher engine speeds than reciprocating piston engines because of the reduced mechanical stresses of the rotating components and the inherent simplicity. However Wankel engines also have higher thermal stresses being continuously heated on one side and cooled on the other. In terms of fuel conversion efficiency, the Wankel engine suffers from the slow, incomplete combustion penalizing the fuel economy.

The latest Mazda engines use two-rotor designs each of 654 cm³ for a nominal 1.3 liter total displacement. Originally, the engine had intake ports on the sides and exhaust ports on the housing, but the latest Renesis engine rearranged the exhaust ports also to the sides permitting larger overall ports (Ohkubo *et al.* 2004). In the latest engines, the compression ratio was 10:1 and the engine was delivering better fuel economy and reliability than previous rotary engines. The fuel consumption was however still significant. In one of the most performing versions of the few proposed in the different markets, the Renesis with 6 side ports is delivering 250 HP @ 8,500 rpm and 216 Nm of torque @ 5,500 rpm.

Despite significant research and development, combustion is the Achilles' heel of the Wankel. The combustion is wall-initiated by two spark plugs in the housing. This leads to a slow, incomplete combustion of the air-fuel mixture, particularly towards the leading and trailing edges of the rotating chamber, with a large amount of unburned hydrocarbons released into the exhaust and a limited pressure build up.

The leading edge of the combustion chamber is travelling in the same direction of one flame front, and the net flame speed is therefore reduced. But is the trailing edge of the combustion travelling against another flame front, for theoretically a much larger net flame speed, that suffers of incomplete combustion, because of the over pressure build up on this side. The trailing side of the rotary engine's combustion chamber develops a squeeze stream which pushes back the flame front.

Being combustion temperatures and pressures also lower than in traditional four-stroke engines

with reciprocating pistons, with thickness of the combustion chamber reducing to zero at the trailing and leading edge, the combustion is hardly complete.

Combustion is much better with hydrogen. Mazda developed and commercialized a bi-fuel gasoline-hydrogen Wankel engine in 2006 (www.mazda.com/stories/rotary/hre/about). Being hydrogen extremely flammable and requiring far less energy to ignite than gasoline, the combustion downfalls were significantly mitigated.

Hydrogen in an ordinary reciprocating piston engine is very vulnerable to abnormal combustion during the intake stroke due to the high temperature of the spark plugs. The rotary engine is very interesting for burning hydrogen being the intake chamber separated from the combustion chamber minimizing the risks of abnormal combustion and being peak temperature and pressure relatively low if compared to reciprocating piston engines.

In the dual-fuel development, the gasoline fuel was port delivered while the hydrogen fuel was directly injected, with minimal engine modifications required vs. the baseline gasoline engine to run dual-fuel.

The dual fuel hydrogen gasoline RX8 is presented in (www.mazda.com/stories/rotary/hre/about). The dual fuel RX8 hydrogen RE of 2006 was able to run on gasoline or hydrogen simply switching from the port fuel injected gasoline to the directly injected hydrogen. One hydrogen injector per rotor was located on top of the injector housing. The dual-fuel system used on-board hydrogen and gasoline. The leasing of the RX-8 Hydrogen RE started in February 2006. The performances of the car were very close with gasoline or hydrogen. However, the dual fuel gasoline and hydrogen car suffered of a significant loss of performance vs. the gasoline only production car.

This paper proposes here a coupled fluid dynamic and detailed chemical kinetics simulations for a jet ignition version of a single fuel hydrogen Wankel engine. The jet ignition device is intended to address the slow and incomplete combustion issues that have penalized so far the Wankel. The spark plug is replaced by a jet ignition device. The jet ignition device is a small pre-chamber connected to the main chamber by calibrated orifices and accommodating a spark plug and a fuel injector (active design) (Boretti and Watson 2009a, b, Boretti 2010a, Boretti *et al.* 2010).

In the passive design, popular with large gas engines working with a homogeneous, premixed charge (Roethlisberger and Favrat 2002a, b), there is no need of the pre chamber injector as the main chamber premixed stoichiometric air fuel mixture enters the pre chamber and it is ignited there. This simplified design is possible with the stoichiometric homogeneous Wankel as it is shown here. As the hydrogen Wankel engine investigated runs premixed homogeneous, the active pre-chamber (with a pre-chamber direct injector and a spark plug) may be replaced by a passive pre-chamber (with a spark plug but no direct injector in the pre-chamber).

Passive pre-chamber are popular in large homogeneous gas engines. Roethlisberger and Favrat (2002a, b) consider the operation of a cogeneration internal combustion engine with non-scavenged pre-chamber ignition. Through the generation of gas jets in the main chamber, the use of a pre-chamber strongly intensifies and accelerates the combustion process. The design reduces the pollutant formation and improves the fuel conversion efficiency even if this claim is more controversial as the heat losses especially in the pre-chamber are larger even if the pressure build-up in the main chamber is much quicker.

The design of jet ignition pre-chambers has traditionally evolved through the use of computational fluid dynamic (CFD), both in the active design (Boretti and Watson 2009a, b, Boretti 2010a) and the passive design (Heyne *et al.* 2011). The coupled CFD and detailed

chemistry approach is possibly the best opportunity to improve knowledge of the phenomena affecting the engine operation prior of experiments (Boretti 2010a).

Small passive pre-chamber spark plugs are off-the-shelf products for gas engines ([www.altronicinc.com/pdf/ignitionaccessories/PPCSP 6-12.pdf](http://www.altronicinc.com/pdf/ignitionaccessories/PPCSP%206-12.pdf)). These passive pre-chamber spark plugs for natural gas-fuelled engines dramatically reduces in-cylinder misfire associated with lean air/fuel ratio operation, light load, and/or low fuel gas heating value. These devices reduce the engine fuel consumption by improving the speed of combustion through flame-jet ignition with simple installation and operation with no independent fuelling system required.

The optimal engine in an Unmanned Aerial Vehicle (UAV) is a light, powerful, compact, silent, reliable and low fuel consumption engine. The lightest engine for a given power is the one with the best power to weight ratio. After the turbine engine, the best internal combustion engines are the two-stroke and the Wankel engine having significant advantages vs. the four stroke engines. The two-stroke engine has one power stroke per crankshaft revolution, while the four-stroke engine only has a power stroke every two revolutions of the crankshaft. The Wankel has three power strokes per rotor revolution, and as the eccentric must rotate three times the rotor speed, similarly to the two strokes the Wankel has one power stroke per crankshaft revolution.

If the most reliable engine is the one with the lesser moving parts in thermal and mechanical stress, then the two stroke and the Wankel engines both have advantages vs. the four stroke engines. In terms of fuel consumption, four stroke engines generally have a better fuel conversion efficiency, as the gas exchange and/or the combustion process are much more difficult in the two strokes or the Wankel engine. However, for UAV applications, as four stroke engines are much heavier, the efficiency gap drastically reduces.

Crank case scavenged two stroke engines issues with lubrication have been solved by using direct injection and precise oiling, however the symmetric port timing, the simultaneous intake and exhaust processes and the limited compression and expansion strokes still keep the fuel conversion efficiency much smaller than the one of four stroke engines. Wankel engines have issues with sealing, but more than that suffer of incomplete and slow combustion for the low temperature and pressures and the thin, rotating combustion chamber. As an additional advantage, the Wankel is fully rotating, while the two or four stroke engines are both mostly reciprocating.

2. Modelling the jet ignited Wankel engine

A jet ignited Wankel engine may be built by using active or passive pre-chambers. Either case rather being low energy wall ignited, the main chamber mixture is bulk ignited by the hot reacting gases issued from the pre-chamber that are rich in radicals and travel high speed all the main chamber. In the engine, direct injection for the main chamber fuel is necessary to avoid the gaseous fuel displacement effects in addition to the intake back-flows important especially for transients, and in case of hydrogen, all the abnormal combustion phenomena.

The jet ignition direct injection homogeneous combustion hydrogen Wankel engine may have same efficiency of four stroke piston engines working homogeneous with gasoline or hydrogen fuels while delivering 3 power strokes per rotor revolution (Boretti *et al.* 2015). With the present innovation, the wall initiated combustion by spark plug is replaced by many high energy bulk igniting jets (Boretti and Watson 2009a, b, Boretti 2010a, Boretti *et al.* 2010, Boretti 2011a, b). The jet ignition is achieved in the proposed simulations by locating along the other casing of the Wankel one jet ignition device. The jet ignition device is for now a small pre-chamber allowing for

a spark plug and a direct injector to be accommodated on one side. On the other side, the volume is connected to the main chamber through calibrated orifices.

During compression, the in-cylinder mixture enters the pre-chamber through the orifices (passive pre-chamber). Before the spark discharge, when working with very lean mixtures, the pre-chamber injector injects the extra fuel needed to make the pre-chamber mixture slightly rich. If the main chamber mixture is stoichiometric, there is no need to use the pre-chamber injector. After the spark discharge occurs, the pre-chamber mixture starts to burn thus raising the temperature and the pressure within the pre-chamber. Multiple jets of hot reacting gases partially burned and with a significant amount of radicals then enter the combustion chamber at high speeds bulk igniting the combustion chamber mixture almost instantaneously across the chamber. This translates in a rapid heat release and a significant pressure and temperature build up.

This general understanding of the possible operation of a jet ignition device when fitted to a Wankel engine is similar to the computed and experimentally tested operation in reciprocating piston engines. However, Wankel and reciprocating piston engines are different, and the design of the jet ignition device may follow these differences, as we learned from the CFD simulations. In the specific of the rotary application, the location of the jet ignition pre-chamber and the timing of the spark starting the combustion process vs. the position of the rotor has to be optimized carefully, as the jets issued in the direction of rotation and against the direction of rotation may experience very different conditions, and consequently they may travel much slower or faster in the different directions.

2.1 CAE model details

CAE engine performance simulation results have been obtained by using a commercial CAE engine performance simulation code, GT-SUITE (www.gtisoft.com). The engine performance simulation results are what needed to assess the suitability of a design alternative in terms of performances. CAE results are ultimately also needed to set up intake and exhaust boundary conditions of the CFD model to produce realistic main chamber conditions at the start of the compression for each lobe. The GT-SUITE code as all the others major performance simulation codes may only permits straightforward descriptions of traditional two and four stroke engines and not of Wankel engines.

In Boretti, Jiang and Scalzo (2015), the engine modeled in GT-SUITE is a 1.3 liter twin-rotor Mazda RX-8 Renesis multi-side ports delivering power of 250 HP @ 8,500 rpm and 216 Nm of torque @ 5,500 rpm. All the engine data have been collected from a purchased Mazda RX-8 vehicle and are therefore not of same quality of the CAD data traditionally used for engine performance model development. The Wankel engine is not one engine type supported by commercial engine performance simulation codes, and an equivalent model has therefore been developed (Boretti *et al.* 2015). Every rotor chamber of the Wankel is modeled as a two stroke equivalent reciprocating piston engine. The twin-rotor engine is modeled as a V6 engine two strokes with reciprocating pistons. This requires the use of fake intake and exhaust junction splits from one pipe to Wankel rotor to three pipes equivalent two stroke reciprocating piston engine cylinders (Boretti *et al.* 2015). This model is tuned to produce the measured volumetric efficiency and torque vs. rpm at wide open throttle.

In the Wankel rotor, a single pipe is available for the intake and exhaust of the three rotor chambers. In this pipe, the flow is rather uniform having every intake or exhaust about 120 degrees crank angle duration, with phases shifted of 120 degrees each other to cover the 360 degrees of

Table 1 Parameters of the high power RENESIS engine

Engine	RENESIS
Version	High-Power
Displacement (cm ³)	654 × 2
Eccentricity × Generating Radius × Width (mm)	15 × 105 × 80
Intake Type	Side Intake
Exhaust Type	Side Exhaust
Compression ratio	10
Timing Primary Intake Port	
Intake Opening (ATDC)	3°
Intake Closure (ABDC)	65°
Timing Secondary Intake Port	
Intake Opening (ATDC)	12°
Intake Closure (ABDC)	36°
Timing Auxiliary Intake Port	
Intake Opening (ATDC)	38°
Intake Closure (ABDC)	80°
Timing Exhaust Port	
Exhaust Opening (BBDC)	50°
Exhaust Closure (BTDC)	3°
Intake System	S-DAIS
Intake Charge Type	Naturally Aspirated

one rotor rotation. Conversely, for every two stroke reciprocating piston engine cylinder every intake or exhaust of about 120 degrees crank angle duration is then followed by 240 degrees of pressure pulsations but no flow.

While the compression ratio is set equal to the actual ratio of 10:1, “*equivalent*” bore and strokes are prescribed, and the piston motion is user imposed to deliver the expected in-cylinder volume versus crank angle. The bore and stroke values are arbitrary and some adjustments of these and the other “*non-physical*” parameters have been necessary to match the experimental power and torque curve working stoichiometric with gasoline. The equivalent bore is assumed to be 84 mm.

The information related to the modeling of the baseline engine has been obtained from Ohkubo *et al.* (2004) and it is summarized in Table 1. The additional information has been inferred from a purchased Mazda Rx-8 vehicle. The details of the high power Renesis engine design are presented in Ohkubo *et al.* (2004). The high-power Renesis has three intake ports per rotor: primary, secondary and auxiliary intake port (six intake ports in total on the two rotors). Their opening and closing timings are different. There is no overlapping of intake and exhaust. A variable intake system S-DAIS High power 3750 rpm and 7250 rpm plus S-DAIS operation strategy are used. The S-DAIS controls the intake manifold length and intake closing timing according to the engine speed, getting maximum dynamic boost effects.

The CAE model is only intended for the study of the differences spark or jet ignition, and gasoline, hydrogen and compressed natural gas fuels could have on the engine performances relative to the spark plug gasoline. The different combustion rates are an input of the model. The combustion is modelled through a Wiebe function with parameters combustion angle 10-90% mass

fraction burned, anchor angle 50% mass fraction burned, and exponent. It is worth mention that as the anchor angle has to be adjusted for the optimum brake torque output, the iterative procedure for determining the combustion parameters may suffer significant inaccuracies. However, a large error on the angle 10-90% mass fraction burned translates in much smaller errors on the brake torque output. The completeness of combustion is also prescribed in the CAE model.

In the CAE model, combustion is set through a Wiebe function where the 10-90% combustion duration, the anchor angle for 50% fuel burned and the Wiebe exponent are set and not computed. The completeness of combustion is also prescribed. In Boretti *et al.* (2015), the combustion parameters are set by using the results of past computational and experimental experiences on reciprocating piston engines (Boretti and Watson 2009a, b, Boretti 2010a, Boretti *et al.* 2010, Boretti 2011a, b), as well as novel, specific Wankel engine simulations with a CFD tool that couples the fluid dynamic to a detailed chemical kinetics model. These latter simulations have not been performed on the true geometry, that is quite complex, but on a simplified geometry to preliminarily test the improvements in the rate of combustion that a jet ignition device may offer vs. a spark plug. Results for the 1.3 liter twin-rotor Mazda RX-8 Renesis multi-side ports are presented in Boretti *et al.* (2015).

May the Mazda RX-8 Renesis multi-side ports engine experience with or without jet ignition be translated in a rotary engine product for Unmanned Aerial Vehicles (UAV)? The answer is certainly yes, but clearly UAV have different constraints, starting from the displacement of the engine that in the largest Wankel engines for UAV is approximately one half of the Renesis at about 300 cm³, to the radial vs. axial dimension of the rotor, with the radial dimension much smaller and the axial dimension therefore much larger than the Renesis (www.rotronuav.com/engines). Furthermore, in addition or as a substitute to gasoline, Wankel engines for UAV use JP5 / JP8 / JET A1 as fuels.

From a combustion perspective, the ticker combustion chamber is typically ignited for four rather than two spark plugs, in two circumferential locations. In terms of gas exchange, the peripheral ports may be much larger per angle of rotor rotation and therefore effective while the side ports are clearly less efficient. Finally, compression ratios for UAV Wankel engines are typically lower than the 10:1 of the Renesis.

While a twin rotor UAV of 600 cm³ based on the Renesis concept could theoretically produce designed for gasoline 115 HP @ 8,500 rpm, and similarly a single rotor UAV of 300 cm³ based on the Renesis concept could deliver 58 HP @ 8,500 rpm, present UAV products have about 50% less output revving 15% less with heavy Jet fuels. Clearly, there are margins of improvement for the specific power of today UAV Wankel engines, and the adoption of jet ignition may help the gasoline Renesis and more than that the heavy Jet fuels UAV Wankel engines to achieve a faster and more complete combustion, ultimately translating in larger specific power and increased fuel conversion efficiency.

2.2 CFD model details

The geometry of an actual engine rotor is quite complex. Therefore, preliminary simulations have been performed on a simplified geometry mathematically generated.

CFD simulations (by using STAR-CCM (www.cd-adapco.com/products/star-ccm-plus)) have then been performed by using a simplified Wankel engine geometry, to easily cope with the description of the three rotating chambers per rotor receiving inflow, developing combustion and distributing the outflow per rotor revolution, and accommodating the jet ignition pre-chamber on

the outer case, as the true engine geometry is much more complicated and it requires more considerable effort.

Star-CD and Star-CCM (www.cd-adapco.com/sites/default/files/brochure/pdf/8017.pdf) are the world leader software products for Computational Fluid Dynamic (CFD) internal combustion engine simulations, extensively used by almost all the Original Equipment Manufacturer (OEM) research and development centers to study and optimize many engines over the last decades. The applications have been supported by extensive validation from the software developer and the customer. The leading author of the paper in particular has been working on Star applications to internal combustion engines since the end of the 1980s within the Fiat group, with applications to production and racing engines, gasoline port fuel injected, gasoline direct injection, diesel pre-chamber and diesel direct injection, all supported by significant experimental evidence.

Even if the model development here is not supported by same experimental evidence of industrial applications, nevertheless, the best practice assumptions adopted for model definition (choice of the governing model equations, discretization scheme, grid size, time integration stepping and scheme) suggest the results are reliable in terms of qualitative comparisons between different ignition strategies. Clearly, the development of the final product may only follow a carefully defined experimental campaign, where the model may also be updated to reflect the further information made available by the experiments.

The present paper only suggests the opportunity to achieve much faster combustion rates in a Wankel engine featuring bulk jet ignition rather than wall initiated spark ignition, and some indications of the location and direction of the jets to deliver the best results.

The Turbulence Model predicts velocity fluctuations. The standard $K-\varepsilon$ Model is a two-equation model that involves transport equations for the turbulent kinetic energy and its dissipation rate. Terms are added to account for effects such as compressibility. In the two-layer $K-\varepsilon$ model the coefficients in the models are identical, but the model gains the added flexibility of an all y^+ wall treatment. In the realizable $K-\varepsilon$ model with two-layer wall treatment a new transport equation is used for the turbulent dissipation rate ε and a critical coefficient of the model, C_ε^- , is expressed as a function of mean flow and turbulence properties, rather than assumed to be constant as in the standard model.

For the Wankel simulations where the detailed chemical kinetics play a fundamental role as the combustion chamber is thin and rotating and the temperatures and pressures are low the detailed chemical kinetic of DARS is coupled to the STAR-CCM+ CFD simulation. DARS is a simulation tool integrated with STAR-CCM+ for the analysis of complex chemical reactions. DARS CFD is an efficient 0-D solver capable of handling gas phase kinetics and surface reactions including many chemical kinetic models and capable of handling both gas phase chemistry, surface chemistry and soot modeling. For sake of simplicity, simulations have been performed with hydrogen that is the simplest fuel in terms of chemical kinetics, almost always available in gas phase (the hydrogen may be liquid only at extremely low temperatures and very high pressures). The coupling of DARS to STAR-CCM+ is described in www.cd-adapco.com/sites/default/files/Presentation/DARS.pdf.

The flow is considered turbulent, compressible, reacting, multi species. Turbulence is modeled by using a Reynolds-Averaged Navier-Stokes (RANS) turbulence model; in particular 2 equations $K-\varepsilon$ model with a two layer all y^+ wall treatment (www.cd-adapco.com/products/star-ccm-plus). The $K-\varepsilon$ RANS model is preferred for simplicity, generality and reliability.

Kinetics equations are obtained by using DARS-CFD (www.cd-adapco.com/sites/default/files/Presentation/DARS.pdf). The kinetics equations of the 21

elementary step mechanism used here are presented in Table 2 (Boretti 2010b). A , n and E_a are the Arrhenius rate constants:

$$k = A \cdot T^n \cdot e^{-E_a/R \cdot T}$$

where T is the temperature and R the gas constant.

Transport and diffusion equations are solved for the nine chemical species, namely for O_2 , H_2 , H_2O , H , O , OH , HO_2 , H_2O_2 . STAR-CCM solves the Partial Differential Equations (PDEs) for energy and species conservation (www.cd-adapco.com/products/star-ccm-plus):

$$\begin{aligned} \frac{\partial}{\partial t} \rho Y_k + \frac{\partial}{\partial x_j} (\rho \cdot u_j \cdot Y_k + F_{k,j}) &= 0 \\ \frac{\partial}{\partial t} \rho h + \frac{\partial}{\partial x_j} (\rho \cdot u_j \cdot h + F_{h,j}) &= \frac{\partial}{\partial t} p + u_j \cdot \frac{\partial}{\partial x_j} p + \tau_{i,j} \cdot \frac{\partial}{\partial x_j} u_i \end{aligned}$$

where t is the time, x_j are the spatial coordinates, ρ is the density, h is the enthalpy, p is the pressure, u_j are velocity vector components, Y_k are the species mass fractions, $F_{k,j}$ are species diffusion vector components, $F_{h,j}$ are enthalpy diffusion vector components and $\tau_{i,j}$ are stress tensor components.

DARS-CFD solves the Ordinary Differential Equations (ODEs) for chemical kinetics (www.cd-adapco.com/sites/default/files/Presentation/DARS.pdf):

$$\frac{\partial}{\partial t} Y_i = \frac{\omega_i}{\rho}$$

where ω_i is the species production rate.

When chemical kinetics is the limiting factor of the reacting system under investigation, near-perfect mixing of reactants and products is usually achieved. However, normally these mixing mechanisms have to rely on fluid motion or large-scale eddies and turbulence to provide the mixing. Local turbulence is particularly important as it promotes micro-scale mixing among the gas species. If the turbulence is too weak to provide fast mixing among the gas species, the micro-mixing process will interfere with the chemical kinetics. The previous model already implicitly addresses both situations. However, to further strengthen the kinetic-turbulence interactions, following Lehtiniemi (2007) the Kong-Reitz model there described is used to scale the previously defined reaction rates s_i through a function of the kinetic and mixing times τ_{kin} and τ_{turb} given as follows:

$$s_i^t = s_i^l \frac{\tau_{kin}}{\tau_{kin} + f \cdot \tau_{turb}}$$

where

$$\tau_{turb} = C \cdot \frac{K}{\varepsilon}$$

with C a constant, K the turbulence kinetic energy and ε the turbulence dissipation rate, while

$$\begin{aligned} f &= \frac{1 - \exp(-r)}{0.632} \\ r &= \frac{m_{H_2O} + m_{H_2}}{1 - m_{N_2}} \end{aligned}$$

Table 2 DARS H₂/O₂ kinetic mechanism (units are cm³ mol s cal K)

Reaction		Arrhenius coefficients		
		A	N	E _a
r1f:	H ₂ +O ₂ =2OH	1.700E+13	0.000E+00	1.999E+02
r1b:	H ₂ +O ₂ =2OH	2.223E+10	3.877E-01	1.202E+02
r2f:	H ₂ +OH=H ₂ O+H	1.170E+09	1.300E+00	1.517E+01
r2b:	H ₂ +OH=H ₂ O+H	7.980E+10	9.726E-01	8.200E+01
r3f:	H+O ₂ =OH+O	2.000E+14	0.000E+00	7.029E+01
r3b:	H+O ₂ =OH+O	6.712E+11	3.742E-01	-1.190E+00
r4f:	O+H ₂ =OH+H	1.800E+10	1.000E+00	3.693E+01
r4b:	O+H ₂ =OH+H	7.014E+09	1.014E+00	2.866E+01
r5f:	H+O ₂ +M ₁ =HO ₂ +M ₁	2.100E+18	-1.000E+00	0.000E+00
r5b:	H+O ₂ +M ₁ =HO ₂ +M ₁	6.276E+20	-1.660E+00	2.142E+02
r6f:	H+2O ₂ =HO ₂ +O ₂	6.700E+19	-1.420E+00	0.000E+00
r6b:	H+2O ₂ =HO ₂ +O ₂	2.002E+22	-2.080E+00	2.142E+02
r7f:	H+O ₂ +N ₂ =HO ₂ +N ₂	6.700E+19	-1.420E+00	0.000E+00
r7b:	H+O ₂ +N ₂ =HO ₂ +N ₂	2.002E+22	-2.080E+00	2.142E+02
r8f:	OH+HO ₂ =H ₂ O+O ₂	5.000E+13	0.000E+00	4.184E+00
r8b:	OH+HO ₂ =H ₂ O+O ₂	4.033E+14	7.798E-02	2.972E+02
r9f:	H+HO ₂ = ₂ OH	2.500E+14	0.000E+00	7.950E+00
r9b:	H+HO ₂ = ₂ OH	3.867E+10	7.930E-01	1.544E+02
r10f:	O+HO ₂ =O ₂ +OH	4.800E+13	0.000E+00	4.184E+00
r10b:	O+HO ₂ =O ₂ +OH	2.212E+12	4.189E-01	2.221E+02
r11f:	2OH=O+H ₂ O	6.000E+08	1.300E+00	0.000E+00
r11b:	2OH=O+H ₂ O	1.050E+11	9.591E-01	7.510E+01
r12f:	H ₂ +M ₂ =2H+M ₂	2.230E+12	5.000E-01	3.874E+02
r12b:	H ₂ +M ₂ =2H+M ₂	6.310E+10	7.542E-01	-5.301E+01
r13f:	O ₂ +M=2O+M	1.850E+11	5.000E-01	3.998E+02
r13b:	O ₂ +M=2O+M	4.508E+07	1.115E+00	-1.038E+02
r14f:	H+OH+M ₃ =H ₂ O+M ₃	7.500E+23	-2.600E+00	0.000E+00
r14b:	H+OH+M ₃ =H ₂ O+M ₃	1.808E+27	-3.182E+00	5.073E+02
r15f:	H+HO ₂ =H ₂ +O ₂	2.500E+13	0.000E+00	2.929E+00
r15b:	H+HO ₂ =H ₂ +O ₂	2.956E+12	4.053E-01	2.292E+02
r16f:	2HO ₂ =H ₂ O ₂ +O ₂	2.000E+12	0.000E+00	0.000E+00
r16b:	2HO ₂ =H ₂ O ₂ +O ₂	5.131E+13	-1.776E-01	1.553E+02
r17f:	H ₂ O ₂ +M=2OH+M	1.300E+17	0.000E+00	1.904E+02
r17b:	H ₂ O ₂ +M=2OH+M	2.622E+09	1.630E+00	-3.268E+01
r18f:	H ₂ O ₂ +H=HO ₂ +H ₂	1.600E+12	0.000E+00	1.590E+01
r18b:	H ₂ O ₂ +H=HO ₂ +H ₂	7.375E+09	5.829E-01	8.682E+01
r19f:	H ₂ O ₂ +OH=H ₂ O+HO ₂	1.000E+13	0.000E+00	7.531E+00
r19b:	H ₂ O ₂ +OH=H ₂ O+HO ₂	3.144E+12	2.556E-01	1.453E+02

and m mass fractions of the relevant species.

Simulations have been performed by using hydrogen as the fuel. Hydrogen is the best fuel for the Wankel. In piston engines, hydrogen typically produces pressures and temperatures that are by

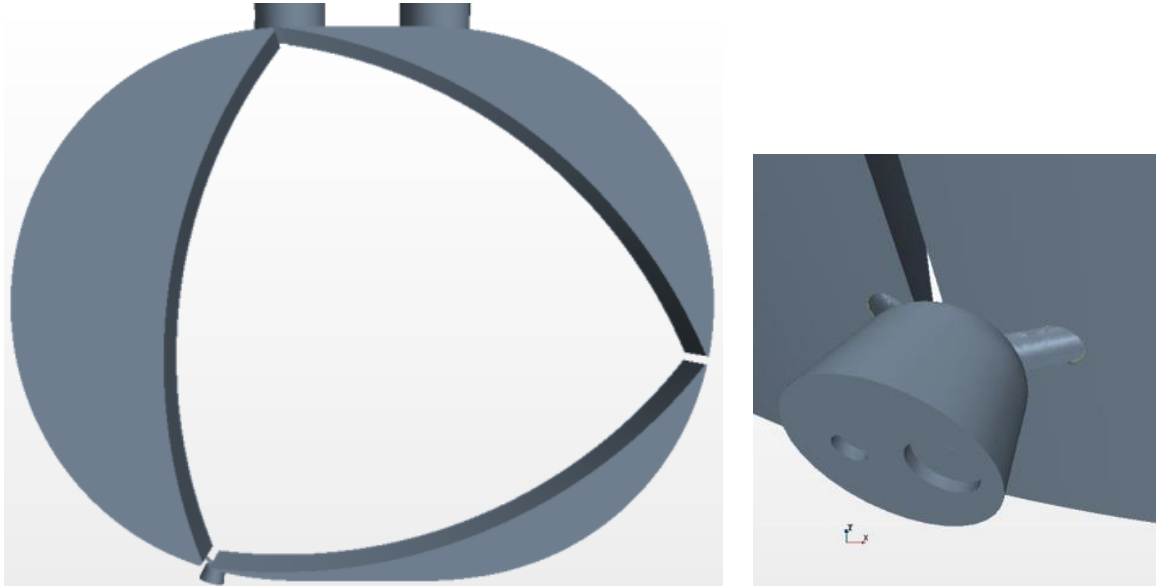


Fig. 1 Simplified Wankel rotor geometry. The details of the jet ignition device are not optimized to deliver the best performances on the specific geometry

far too high when working stoichiometric. In the Wankel, where the pressures and temperatures are typically lower than in piston engines, the largest than gasoline peak temperature and pressure working stoichiometric are not an issue. Furthermore, combustion with hydrogen is typically much faster than with other fuels and this also helps the otherwise slow combusting Wankel. However, the main reason why preliminary simulations have been performed by using hydrogen is that the chemical kinetics of hydrogen air mixtures is much simpler, and hydrogen does not have the issue of the liquid injection requiring further special modeling additions.

In the model, the hydrogen is premixed with air at the intake. The firing top dead center is 45 degrees rotor angle from the start position. Therefore, the three firing TDC for a rotor revolution are 45, 165 and 285 degrees rotor angle. More than one single lobe combustion can be easily computed. While spark ignition is modeled by using a small ignition volume along the casing where the spark plug is located, the jet ignition is modeled by placing this small ignition volume along the surface of the jet ignition device where the spark plug is located.

3. Computational results

The operation of the jet ignition device is described first by using the CFD tool.

Fig. 1 presents the rotor geometry detailing the 3 lobes and the casing, plus the (equivalent) intake and exhaust pipes where intake and exhaust boundary conditions are set, and the jet ignition device. Fig. 2 presents the computational grid. In the simulations proposed here after, there is no additional injection of fuel in the pre-chamber, so the injector head is modeled as solid wall. The spark plug electrode has on top a small sphere where the spark discharge is simulated by increasing the temperature to 2500 K over the spark duration. Fig. 3 presents the pressure evolution, Fig. 4 the temperatures and Fig. 5 the fuel mass fraction.

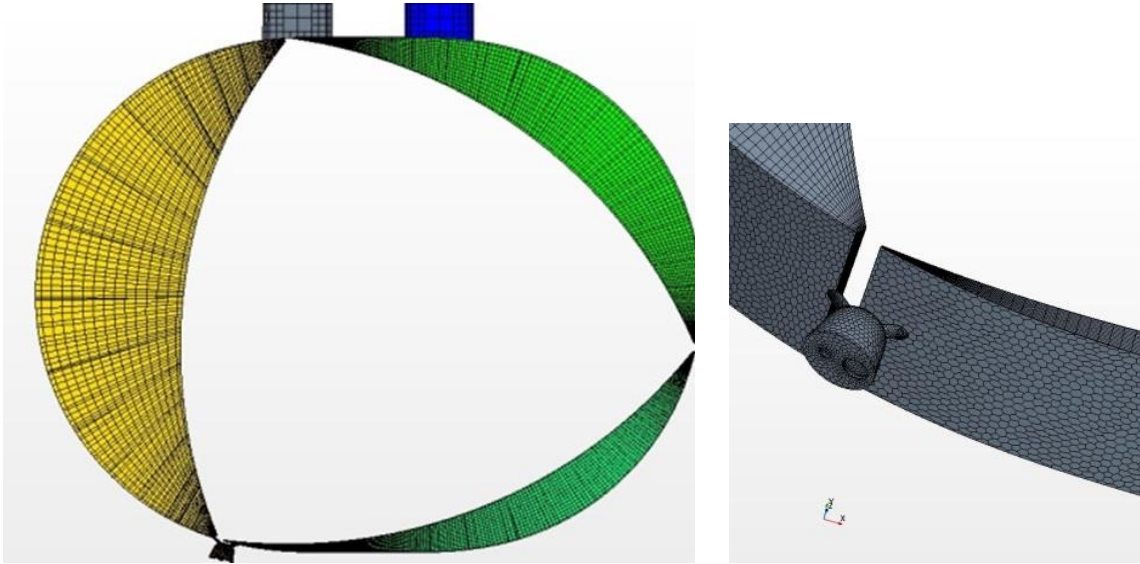
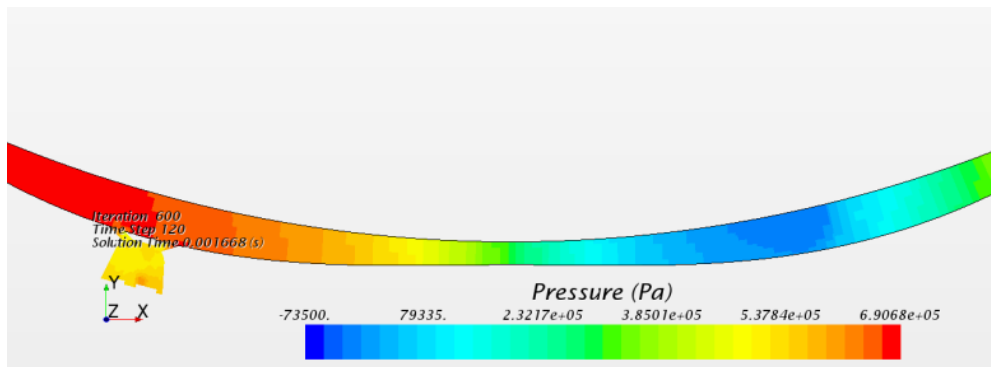
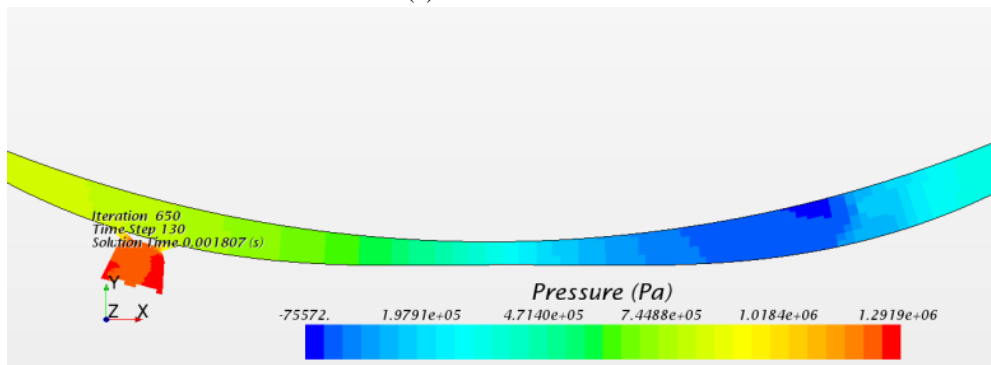


Fig. 2 Computational grid. The details of the computational mesh are not optimized to deliver the best simulation results on the specific geometry

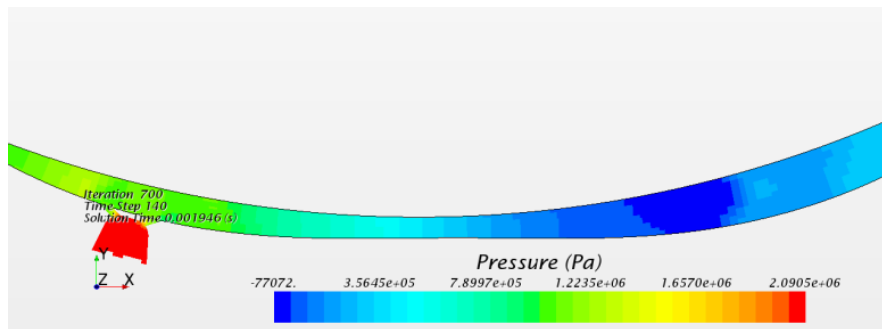


(a) time=1.668 ms

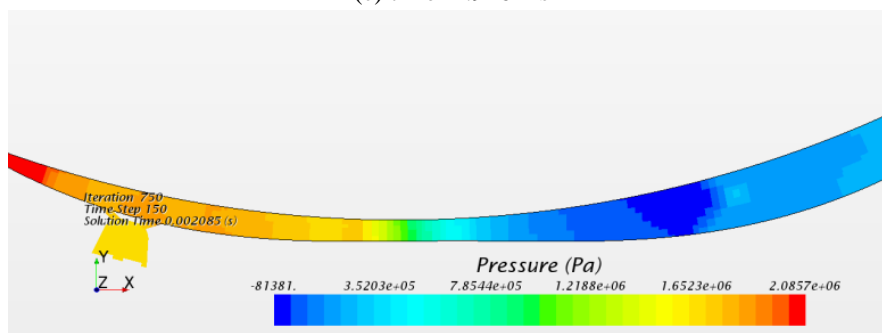


(b) time=1.807 ms

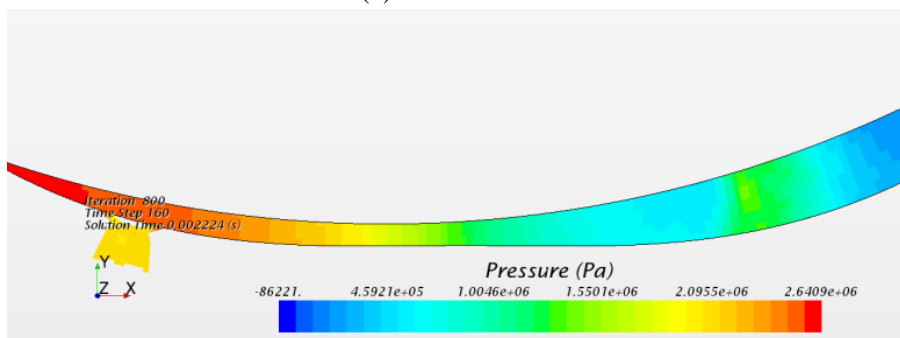
Fig. 3 Pressure evolution during combustion and expansion. As shown in the hydrogen profile of Figure 5, combustion starts in the pre-chamber at the spark plug electrodes (a), then extends to the entire pre-chamber (b)



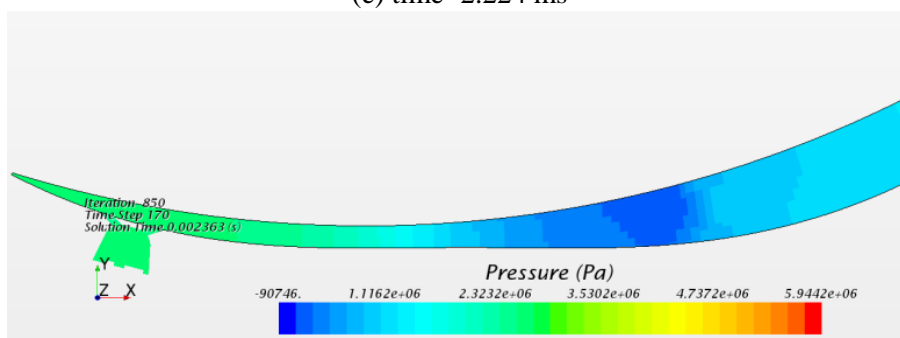
(c) time=1.946 ms



(d) time=2.008 ms



(e) time=2.224 ms



(f) time=2.363 ms

Fig. 3 Continued. Pressure evolution during combustion and expansion. As shown in the hydrogen profile of Figure 5, finally ignites the main chamber mixtures with flame propagating faster in the direction of rotation (d), the flame front moves very rapidly towards the leading edge of the combustion chamber (e, f)

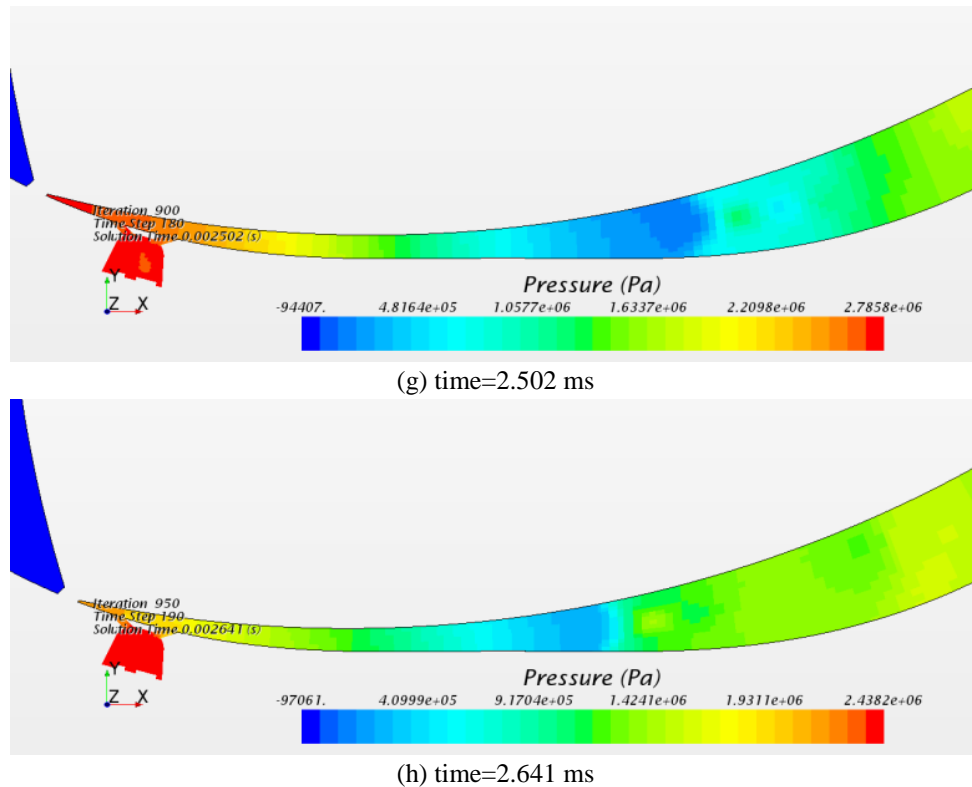
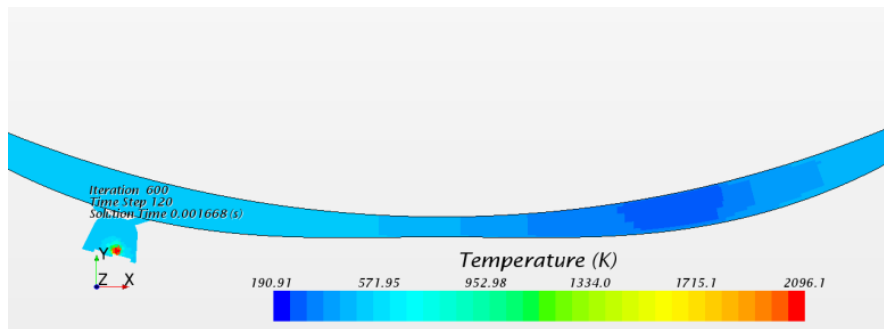


Fig. 3 Continued. Only a small amount of fuel is left to burn at the trailing edge of the combustion chamber (g) and combustion is finally completed (h). The temperature field follows the release of energy and the gas expansion

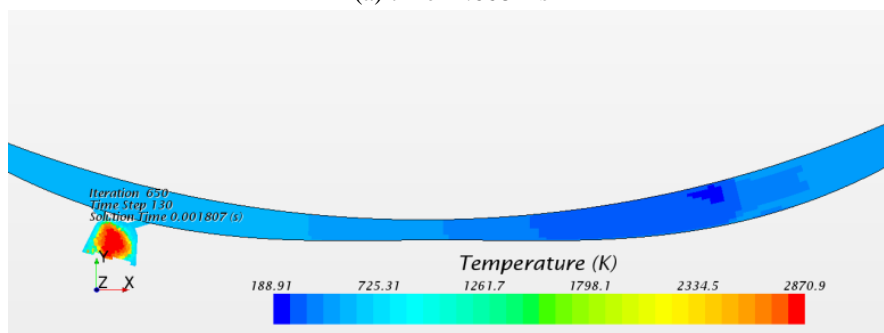
The hydrogen direct injector (main chamber) is not represented, as an equivalent premixed air fuel mixture is introduced from the inlet. Being the hydrogen in gas state, there is no problem of wall wetting and vaporization that could make the main chamber mixture non-homogeneous as with liquid fuels. Figs. 3 to 5 present sample results obtained for the full load operation at 6,000 rpm rotor speed. This is an extreme condition (the eccentric speed is three times this speed) to verify that the ignition system is robust under every possible operations.

The pressure evolution is the most important feature to consider when designing the jet ignition device for a Wankel, as the conditions downstream of the nozzles differ considerably from piston engines applications. During compression, the pressures towards the trailing edge are generally much larger. Pressure fluctuations are also superimposed to this general pattern build up. After combustion starts, the pressure build-up within the pre-chamber produces the jet of partially burnt hot gases that travel across the main chamber in both directions. As the pressure on the right is much lower, because combustion is releasing heat on the left and because the volume on the right is expanding, the travel of the jet in the direction of rotation is extremely quick.

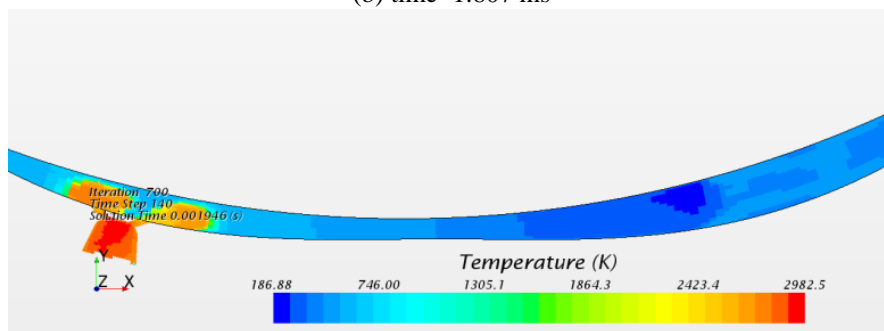
It takes about 1.4×10^{-4} s (or 5 degrees of rotation of the rotor) to have the pre-chamber completely enflamed. Then, in another 1.4×10^{-4} s the jets have ignited a significant portion of the main chamber mixture and the flame is travelling very fast in the direction of rotation. After another 1.4×10^{-4} s, the most part of the main chamber mixture towards the leading edge has been



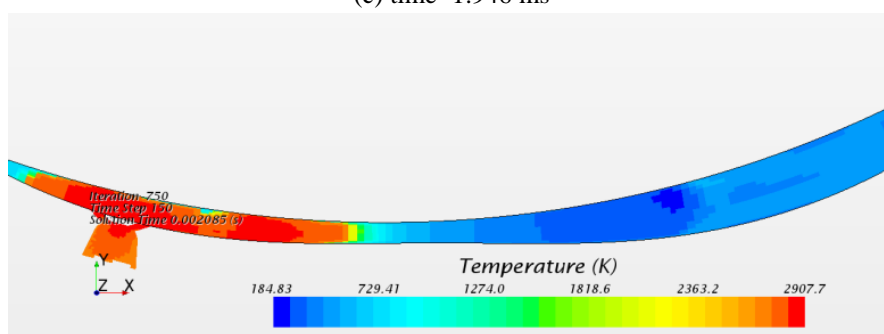
(a) time=1.668 ms



(b) time=1.807 ms

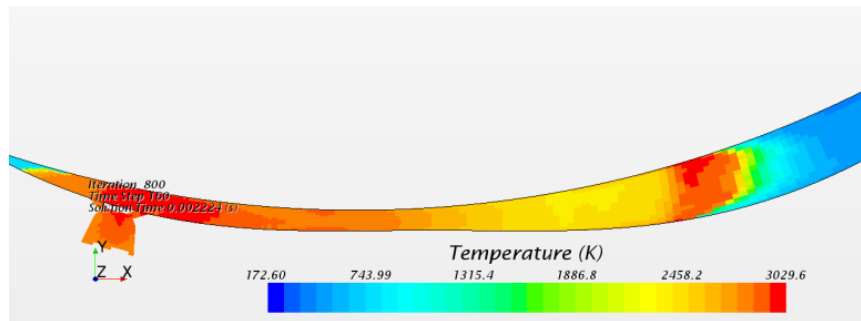


(c) time=1.946 ms

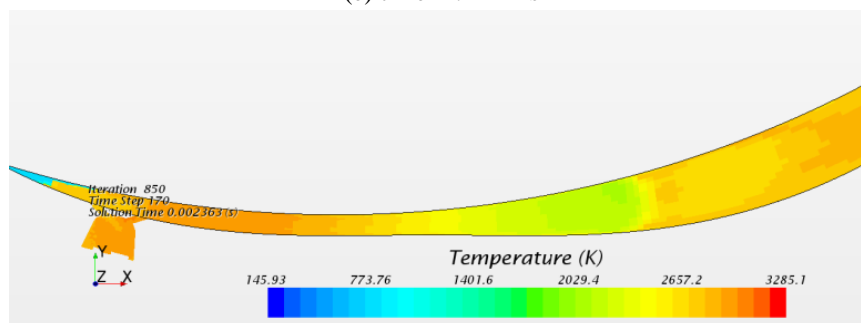


(d) time=2.008 ms

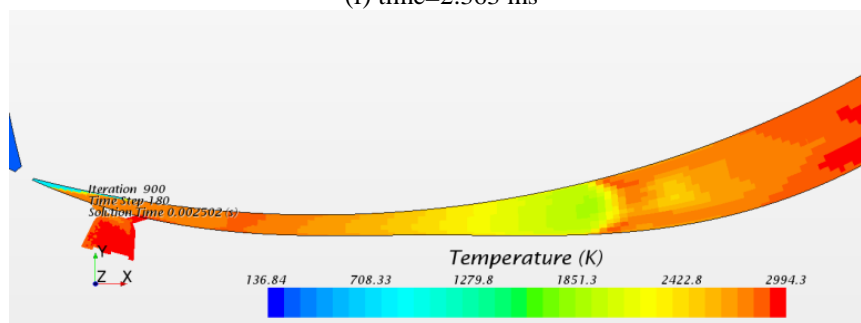
Fig. 4 Temperature evolution during combustion and expansion. As shown in the hydrogen profile of Figure 5, combustion starts in the pre-chamber at the spark plug electrodes (a), then extends to the entire pre-chamber (b) and finally ignites the main chamber mixtures with flame propagating faster in the direction of rotation (d)



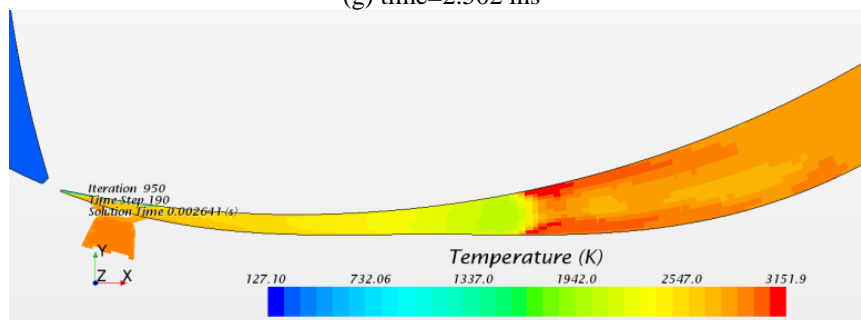
(e) time=2.224 ms



(f) time=2.363 ms

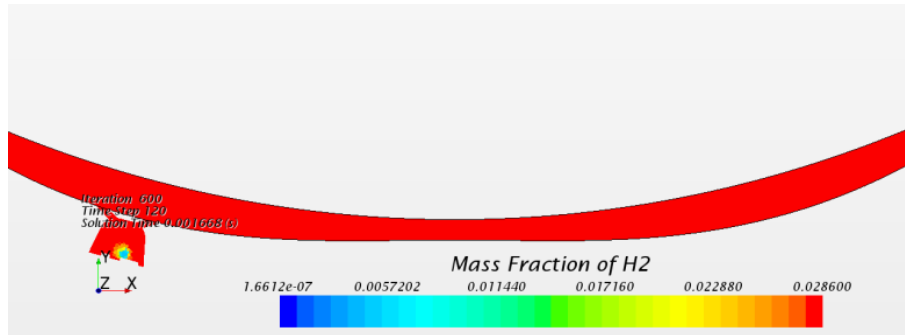


(g) time=2.502 ms

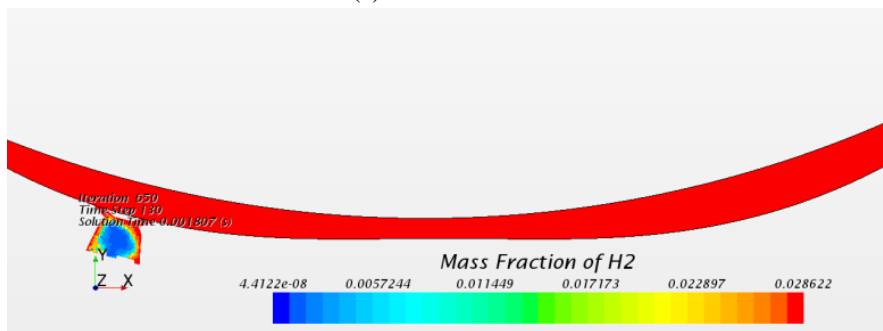


(h) time=2.641 ms

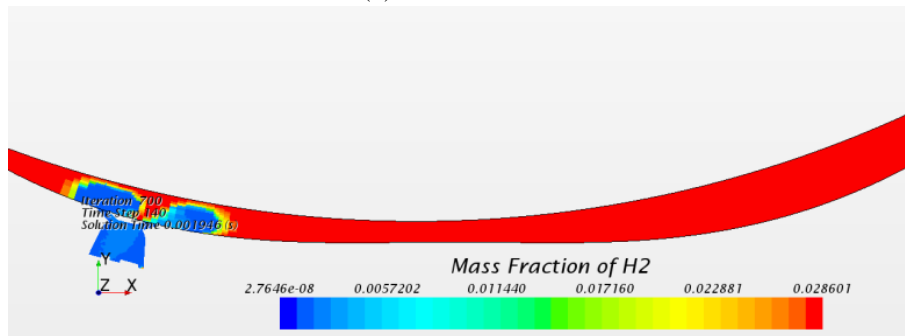
Fig. 4 Continued. Temperature evolution during combustion and expansion. As shown in the hydrogen profile of Figure 5, the flame front moves very rapidly towards the leading edge of the combustion chamber (e, f). Only a small amount of fuel is left to burn at the trailing edge of the combustion chamber (g) and combustion is finally completed (h). The temperature field follows the release of energy and the gas expansion



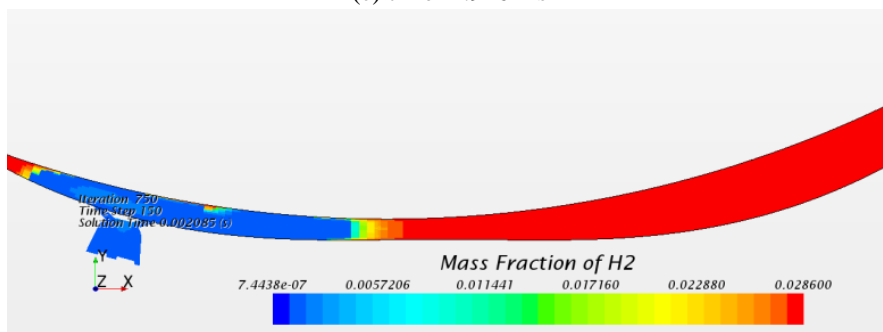
(a) time=1.668 ms



(b) time=1.807 ms

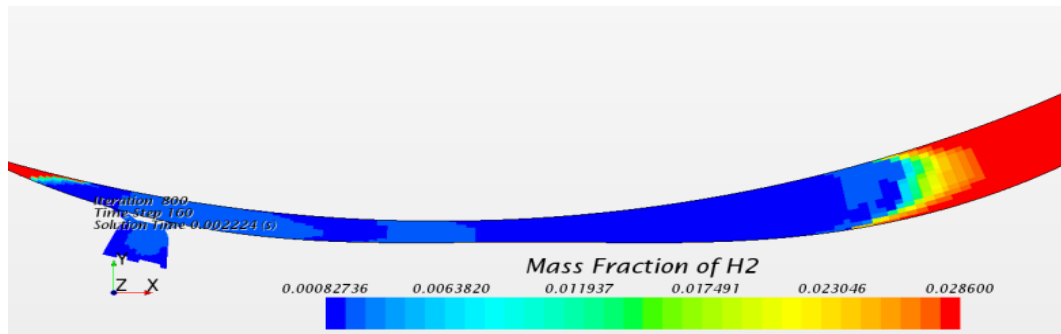


(c) time=1.946 ms

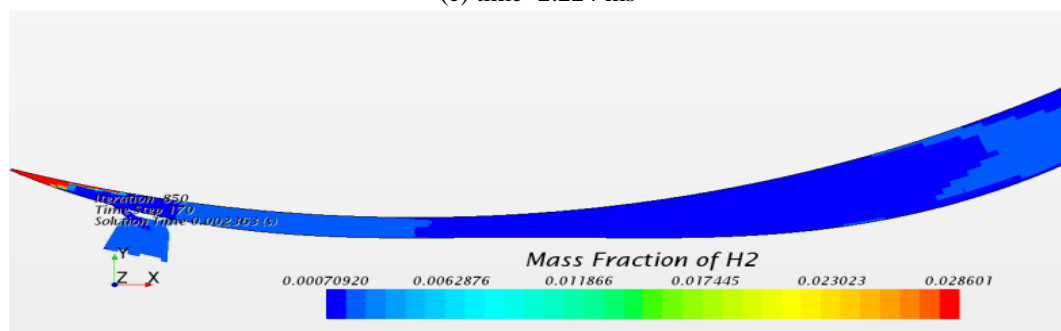


(d) time=2.008 ms

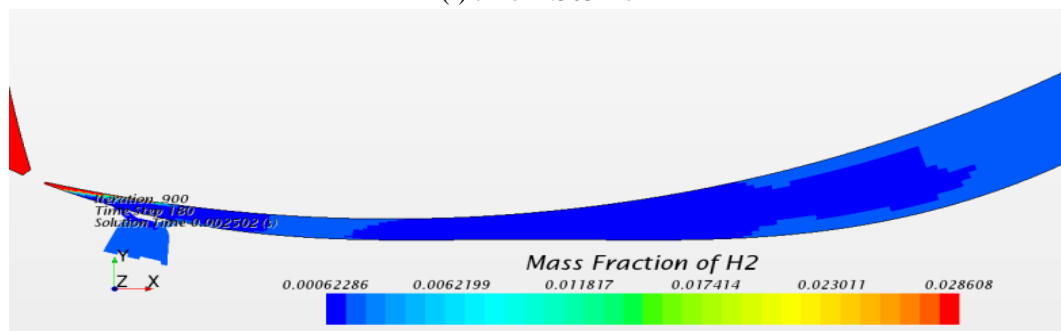
Fig. 5 Hydrogen mass fraction evolution during combustion and expansion. Combustion starts in the pre-chamber at the spark plug electrodes (a), then extends to the entire pre-chamber (b) and finally ignites the main chamber mixtures with flame propagating faster in the direction of rotation (d)



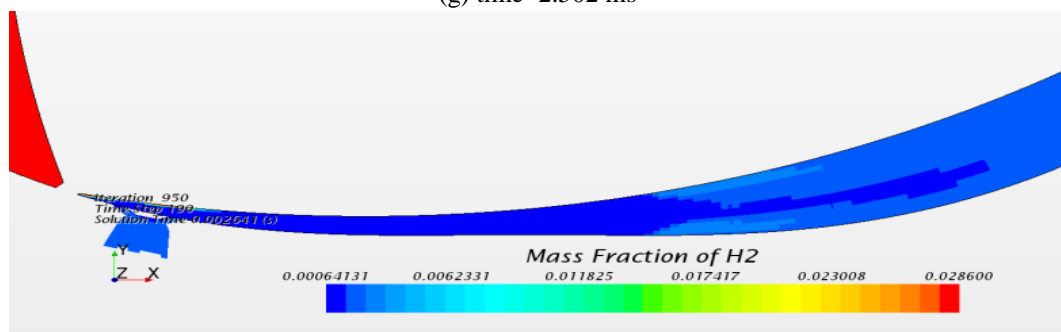
(e) time=2.224 ms



(f) time=2.363 ms

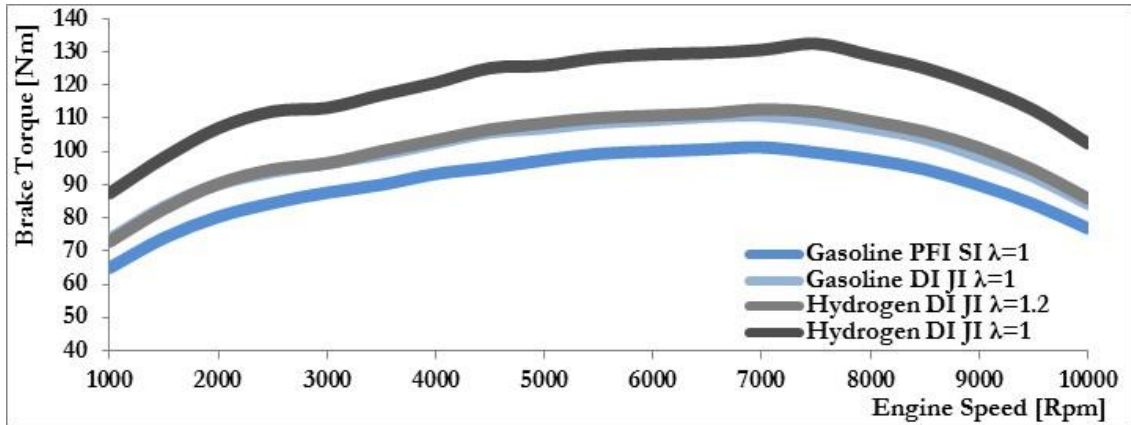


(g) time=2.502 ms

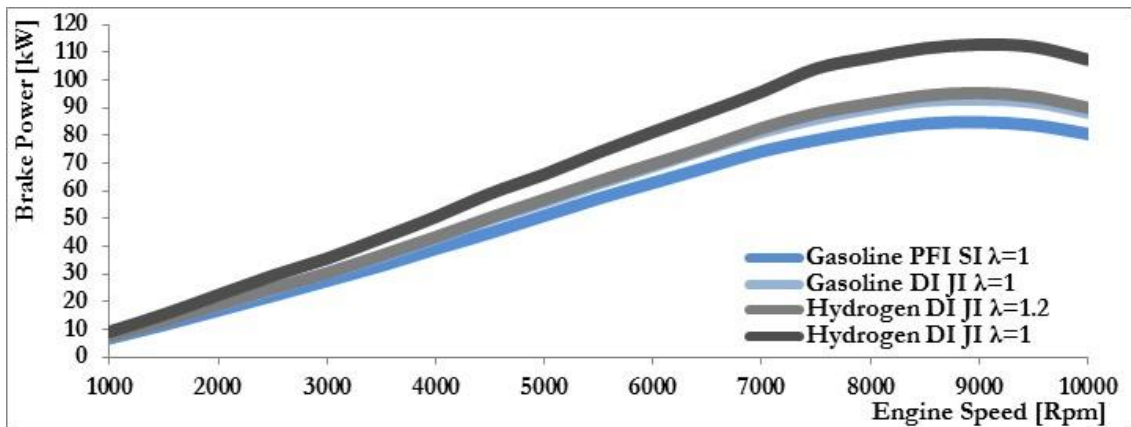


(h) time=2.641 ms

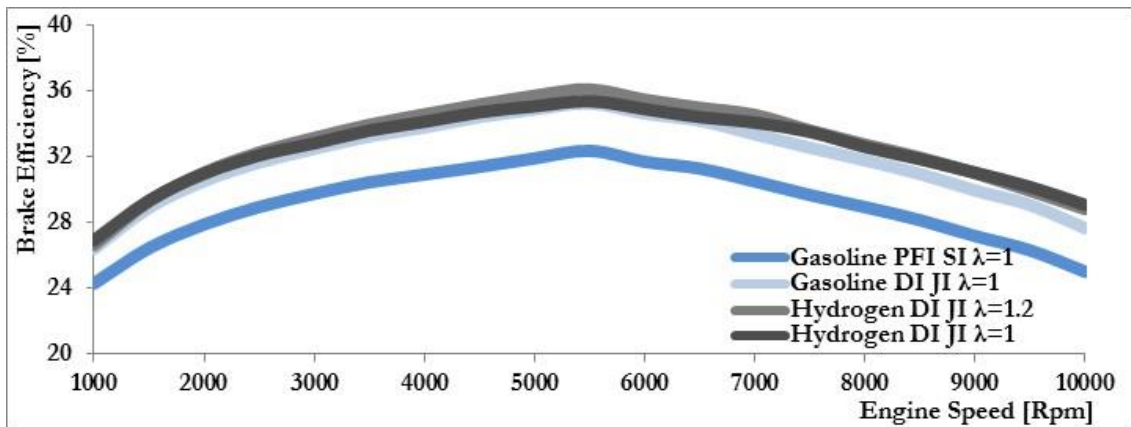
Fig. 5 Continued. Hydrogen mass fraction evolution during combustion and expansion. The flame front moves very rapidly towards the leading edge of the combustion chamber (e, f). Only a small amount of fuel is left to burn at the trailing edge of the combustion chamber (g) and combustion is finally completed (h)



(a)



(b)



(c)

Fig. 6 Computed brake torque, power and efficiency of a 600 cm³ twin rotor Wankel engine. The efficiency is defined as the ratio of engine brake power to fuel flow power. The computed values are only first indication of the performances such an engine could have after careful, specific research and development being the specific design and the CAE and CFD applications non-conventional

reached by the flame, and very little fuel and air mixture is unburned towards the leading as well as the trailing edges. Therefore, the 10-90% combustion duration is close to 10 degrees of rotor angle even at these extreme speeds.

By comparing surface ignition (results not shown here but proposed in Boretti *et al.* 2015) and jet ignition it appears that the combustion duration may be reduced much more than 50%, with the fuel within the main chamber always burning completely with jet ignition, as it is not the case with spark ignition.

As the proposed results are only preliminary, different timings of the spark and different locations of the jet volume and shape of the ignition pre-chamber and the connecting pipes are being investigated. Nevertheless, the CFD simulations suggest the jet ignition may be the key word to make more successful the Wankel engine.

The previous analyses of Boretti *et al.* (2015) and the above paragraphs can be applied to compute a first guess a twin rotor 600 cm³ Wankel engine could have working with spark or jet ignition with gasoline or hydrogen fuels. These results are obviously very speculative as only a specific experimental campaign may provide better insight in the operation of the strongly non-conventional engine.

Fig. 6 presents the computed brake torque, power and efficiency, this latter defined as the ratio of engine brake power to fuel flow power. PFI stands for port fuel injected, DI for directly injected, SI for spark ignition and JI for jet ignition.

The assumptions made to derive the performance these performance figures are summarized below:

- Every rotor of a Wankel engine is modelled as three two stroke engine cylinders in a CAE model (GT-SUITE);
- The parameters of this baseline model are tuned to reproduce the measured volumetric efficiency and brake torque of a twin rotor, double spark ignition, port fuel injected, stoichiometric gasoline 1.3 liter Renesis multiport engine.
- CFD simulations (STAR-CCM+ and DARS) are used to compute the relative combustion evolution with spark and jet ignition in a hydrogen fuelled, stoichiometric, simplified Wankel engine geometry.
- Changes in fuel and ignition method are introduced in the CAE model by simply replacing the port injected gasoline with port or directly injected gasoline or hydrogen, shortening the 10-90% mass fraction burned angle and improving the mass fraction burned in case of jet ignition, and adjusting the anchor angle 50% mass fraction burned for maximum brake torque conditions.
- Operation of a gasoline or hydrogen fuelled single or twin rotor Wankel engine of reduced displacement is obtained by assuming the brake mean effective pressure (torque per unit volume) and the brake fuel conversion efficiency (brake power to fuel flow power) remain the same.

These assumptions make the modelling results certainly less reliable than those that may follow the use of CAE and CFD codes coupled to a proper experimental data base. However, without detailed measurements of small Wankel engines operation supporting the model development there is no opportunity to provide a better guess.

Jet ignition appears to be the key of a 15% peak efficiency improvement, with the traditionally low efficiency of the Wankel. Similar improvements are also obtained in the power and torque outputs.

Non mentioned before, in additional to the non-conventional CAE and CFD computation of indicated parameters and combustion rates, also the computation by correlation of the friction parameters needed to computed the brake parameters may be inaccurate.

4. Discussion

The Star-CD/Star-CCM modelling of combustion in reciprocating piston internal combustion engines has been the subject of numerous validation and application works over the last 25 years, by the author (see for example Boretti *et al.* 1991a, b, 1992a, b) and by many other researchers, mostly in the industry and research centres but also in the academy. The jet ignition of the main chamber mixture has been considered even if in a limited number of cases (see for example Boretti *et al.* 2007). The Wankel validations and applications have not been very common, not only with the Star-CD/Star-CCM family of CFD codes, but also with other CFD products. Therefore, the best practice guidelines defined for reciprocating piston engines not necessarily work well for the Wankel engine having specific requirements that only a detailed validation campaign may sort out. Hence, the proposed model is not certainly an optimised nor a validated one but it is only intended to provide a first estimations of the advantages that jet ignition may give in this kind of engines and develop ideas to test in further developments with coupled experiments and simulations.

As the Wankel rotor model must include the intake and the exhaust to be meaningful, as the unburned hydrocarbons escaping combustion are one of the major parameters to consider, the proposed model is therefore very simple to easily deal with rotor lobe-intake and rotor-exhaust interfaces, with the intake and exhaust ports located along the periphery and not on the sides. A Mazda Rx-8 car equipped with the latest Renexis engine has been purchased with the goal of carrying out engine dynamometer experiments on a standard and a modified version. Funding permitting, the next steps would be to build prototype jet ignition devices same size of the present spark plugs, perform the engine experiments on the baseline and the jet ignition version, and develop a model of one rotor of the Renexis engine to validate first the standard twin spark plug per rotor ignition combustion, and then the simplest jet ignition option replacing the standard spark plugs with jet ignition devices placed in the same locations. Despite this location is not optimal, the overall modelling accuracy will certainly considerably improve following this exercise, and a proper CFD assisted design of the novel rotor architecture featuring a modified casing will follow. At this point, the preliminary proof of concept of the jet ignited Wankel engine will be completed.

The basic CFD model used here was originally developed by CD-Adapco (the developer of Star-CD/Star-CCM) to simulate the gas exchange – but no combustion – in a simplified Wankel geometry (www.cd-adapco.com/ja/printpdf/5946). The model was used to compute the Line Integral Convolution (LIC) plot of velocity vectors representing the flow within the rotor lobes and the intake and exhaust peripheral ports in absence of any reaction. All the boundaries of the computational domain were generated by using simple mathematical equations. The present model was created by replacing the outer casing surface given as a Stereo Litography (STL) file with a CAD generated STL file including the details of the jet ignition pre-chamber, meshing the computational domain with a finer grid and introducing the reacting flow physical model and more proper boundary conditions. By only changing the STL file, a new model is generated with the only extra need to change of the ignitor location, the small volume between the spark plugs electrodes, to produce same quality results.

5. Conclusions

We have shown how Jet Ignition may be the solution to revitalize the Wankel engine suffering of poor combustion applying this concept to a simplified hydrogen Wankel engine. Combustion

when wall initiated with spark plugs is slow and incomplete. The issue may be solved by using jet ignition device. The jet ignition for Wankel engines is not a straightforward solution, as there is no experience at all in the use of jet ignition devices in rotary engines but only in reciprocating piston engines.

As the combustion evolution and the pressure build-up in a Wankel and a piston engine differ considerably, the definition of the optimum jet ignition device requires special attention. From the coupled fluid dynamic and detailed chemical kinetics simulations of gas exchange and combustion in a Wankel engine working with stoichiometric hydrogen air mixtures fitted with a jet ignition pre-chamber we learned that the design of the jet ignition pre-chamber has to evolve differently from the guidelines set for reciprocating piston engines application.

With reciprocating piston engines, the jets issued from the pre chamber have about same properties in any direction. In the Wankel, the jet issued in the direction of rotation of the rotor and against this direction may find very different conditions, as the pressure within a rotor lobe may vary dramatically from leading to trailing edge as a function of the chamber volume and the heat released during combustion.

While a central jet ignition pre-chamber may produce insufficient ignition of the mixture towards the trailing edge, a jet ignition pre-chamber shifted towards the trailing edge produces much quicker combustions despite the longer path to reach the trailing edge mixture, as the jet is moving faster thanks to the trailing edge pressure build up.

References

- Boretti, A.A., Lisbona, M.G. and Nebuloni, P. (1991a), "Numerical modelling of three-dimensional flows within the cylinder of a 4 valve spark ignition engine", *INRIA/SIAM Fourth International Conference on Numerical Combustion*, St. Petersburg Beach, Florida, USA, December.
- Boretti, A.A., Lisbona, M.G. and Nebuloni, P. (1991b), "Numerical modelling of three-dimensional flows within the cylinder of a direct injection diesel engine", *INRIA/SIAM Fourth International Conference on Numerical Combustion*, St. Petersburg Beach, Florida, USA, December.
- Boretti, A., Lisbona, M.G., Nebuloni, P. and Bland, R. (1992a), "Spark-ignition engine combustion chamber design with three-dimensional flow computations", *ATA Third International Conference Innovation and Reliability in Automotive Design and Testing*, Florence, Italy, April.
- Boretti, A. *et al.* (1992b), "Diesel engine combustion chamber design with three dimensional flow computations", *IMEchE Conference on Combustion in Engines*, London, UK, December.
- Boretti, A., Brear, M. and Watson, H. (2007), "Experimental and numerical study of a hydrogen fuelled I.C. engine fitted with the hydrogen assisted jet Ignition system", *Proceedings of the Sixteenth Australasian Fluid Mechanics Conference*, Gold Coast, Australia, December.
- Boretti, A.A. and Watson, H.C. (2009a), "Enhanced combustion by jet ignition in a turbocharged cryogenic port fuel injected hydrogen engine", *Int. J. Hydro. Energy*, **34**(5), 2511-2516.
- Boretti, A.A. and Watson, H.C. (2009b), "The lean burn direct injection jet ignition gas engine", *Int. J. Hydro. Energy*, **34**(18), 7835-7841.
- Boretti, A. (2010a), "Comparison of fuel economies of high efficiency diesel and hydrogen engines powering a compact car with a flywheel based kinetic energy recovery systems", *Int. J. Hydro. Energy*, **35**(16), 8417-8424.
- Boretti A. (2010b), "Modelling auto ignition of hydrogen in a jet ignition pre-chamber", *Int. J. Hydro. Energy*, **35**(8), 3881-3890.
- Boretti, A., Watson, H. and Tempia, A. (2010), "Computational analysis of the lean-burn direct-injection jet ignition hydrogen engine", *Proceedings of the Institution of Mechanical Engineers, Part D: Journal of*

- Automobile Engineering*, **224**(2), 261-269.
- Boretti, A. (2011a), "Stoichiometric H2ICEs with water injection", *Int. J. Hydro. Energy*, **36**(7), 4469-4473.
- Boretti, A. (2011b), "Stoichiometric H2ICE with water injection and exhaust and coolant heat recovery through organic Rankine cycles", *Int. J. Hydro. Energy*, **36**(19), 12591-12600.
- Boretti, A., Jiang, S. and Scalzo, J. (2015), "A novel Wankel engine featuring jet ignition and port or direct injection for faster and more complete combustion especially designed for gaseous fuels", SAE P. 2015-01-0007.
- Danieli, G., Ferguson, C., Heywood, J. and Keck, J. (1974), "Predicting the emissions and performance characteristics of a Wankel engine", SAE P. 740186.
- Heyne, S., Millot, G. and Favrat, D. (2011), "Numerical simulations of a prechamber autoignition engine operating on natural gas", *Int. J. Thermodyn.*, **14**(2), 43-50.
- Izweik, H.T. (2009), "CFD investigation of mixture formation, flow and combustion for multi-fuel rotary engine", d-nb.info/1001122860/34.
- Jones, C. (1979), "A review of curtiss-wright rotary engine developments with respect to general aviation potential", SAE P.790621.
- Lehtiniemi, H. (2007), "Efficient engine CFD with detailed chemistry", *ERC 2007 Symposium Future Fuels for IC Engines*, Madison, June.
- Ohkubo, M., Tashima, S., Shimizu, R., Fuse, S. and Ebino, H. (2004), "Developed technologies of the new rotary engine (RENESES)", No. 2004-01-1790, SAE Technical Paper.
- Roethlisberger, R.P. and Favrat, D. (2002a), "Comparison between direct and indirect (prechamber) spark ignition in the case of a cogeneration natural gas engine, part I: engine geometrical parameters", *Appl. Therm. Eng.*, **22**(11), 1217-1229.
- Roethlisberger, R.P. and Favrat, D. (2002b), "Comparison between direct and indirect (prechamber) spark ignition in the case of a cogeneration natural gas engine, part II: engine operating parameters and turbocharger characteristics", *Appl. Therm. Eng.*, **22**(11), 1231-1243.
- Sherman, D. (2008), "The rotary club", *Autom. Mag.*, February, 76-79.
- Shimizu, R., Okimoto, H., Tashima, S. and Fuse, S. (1995), "The characteristics of fuel consumption and exhaust emissions of the side exhaust port rotary engine", SAE P. 950454.
- Yamamoto, K., Muroki, T. and Kobayakawa, T. (1972), "Combustion characteristics of rotary engines", SAE P. 720357.
- www.altronicinc.com/pdf/ignitionaccessories/PPCSP 6-12.pdf
- www.cd-adapco.com/products/star-ccm-plus
- www.cd-adapco.com/sites/default/files/brochure/pdf/8017.pdf
- www.cd-adapco.com/sites/default/files/Presentation/DARS.pdf
- www.gtisoft.com/
- www.mazda.com/stories/rotary/hre/about
- www.rotronuav.com/engines
- www.cd-adapco.com/ja/printpdf/5946